Received: 28 April 2025 | Revised: 24 June 2025 | Accepted: 2 September 2025 | Published online: 24 September 2025

RESEARCH ARTICLE

Journal of Optics and Photonics Research
2025, Vol. 00(00) 1–13
DOI: 10.47852/bonviewJOPR52026038

BON VIEW PUBLISHING

Performance Analysis of RSA Encrypted Secure Free-Space Optical Communication Link Under Adverse Atmospheric Conditions Implemented on a Testbed

Dhanush Devappa B C[1], Chandani Kashyap[1], Shreyas Jain[1], Soumit Banerjee[1] and Appala Venkata Ramana Murthy[1,*]

[1]*Department of Applied Physics, Defence Institute of Advanced Technology, India*

Abstract: The increasing interest in the field of free-space optical communication (FSOC) can be attributed to the rising demand for an alternate communication system that can replace the existing communication systems. FSOC ranges from a few meters of indoor communication to a few kilometers of terrestrial range to satellite communication. The challenges posed vary in different scenarios. For indoors, major challenges are the artificial light sources, and for outdoors, it is the atmospheric channel-related concerns, such as fog, smoke, wind flow, and the turbulence of the channel. These adverse atmospheric conditions will degrade the link performance. On the other hand, the demand for secure communication links from the physical layer to the network layer is ever-increasing. In this paper, we have conducted a simulation study for various modulation techniques in different atmospheric conditions and have demonstrated the integration of a Rivest–Shamir–Adleman (RSA) encrypted link that offers security along with various digital modulation schemes. We have designed a lab-level setup for FSOC and developed various testbeds to simulate adverse atmospheric conditions. We tested FSOC link performance by measuring the bit error rate with various modulation schemes, that is, OOK (NRZ, RZ), PPM, and DPIM formats, along with RSA on the testbed.

Keywords: optical communication, Rivest–Shamir–Adleman, modulation scheme, atmospheric conditions

1. Introduction

Free-space optical communication (FSOC) is becoming an increasingly demanding technology due to its advantages over conventional counterparts, such as high bandwidth capacity, no licensing issues, ease of installation, etc. At the same time, there is also a demand that FSOC should meet all the communication benchmarks from the network layer to the physical layer with all the modulation, encoding, and encryption standards. Modulation schemes include all sorts of digital modulation techniques like On-Off Keying (OOK), pulse modulation schemes, and differential pulse modulation schemes, and encoding techniques include all error correction codes and other mitigation techniques. Encryption includes symmetric encryption (e.g., Advanced Encryption Standard (AES)) and asymmetric encryption (e.g., Rivest–Shamir–Adleman (RSA) encryption), which will make the FSOC system complete. Then, only the modern-day FSOC serves as a mature alternative to other communication technologies [1, 2]. In its basic form, FSOC uses modulated optical signals to transmit information over atmospheric channels [3, 4]. The major obstacle to these optical signals, while transmitted, might undergo signal losses due to environmental effects like absorption, scattering, scintillation, and turbulence, which can cause the optical beam to weaken, spread, or fluctuate while traveling in free space. This eventually causes loss of data and limits the link performance. The immediate solution to this is to introduce various modulation, mitigation, and encryption techniques to protect these optical signals and ensure an error-free data transfer [5, 6].

Several researchers are making continuous attempts to develop various techniques to understand, investigate, mitigate, and minimize the adverse atmospheric effects and to improve the quality of the optical signal at the receiver to achieve lower bit error rates (BERs) and improve the link performance. One of these techniques is the use of modulation schemes. Modulation techniques offer bandwidth and power efficiency, resulting in high signal-to-noise ratio (SNR) values, thus increasing the reliability of the communication link and reducing the probability of error occurrence [7]. There are various modulation techniques like On-Off Keying Non-Return-to-Zero (OOK-NRZ), On-Off Keying

*Corresponding author: Appala Venkata Ramana Murthy, Department of Applied Physics, Defence Institute of Advanced Technology, India. Email: avrmurthy@diat.ac.in

Return-to-Zero (OOK-RZ), Pulse Position Modulation (PPM), Differential Pulse Interval Modulation (DPIM), Differential Phase-Shift Keying (DPSK), etc., each of which is efficient in its own way. Performance of different modulation schemes in free-space optical transmission was done by Sangeetha et al. [8], where they focused on M-ary quadrature amplitude modulation (M-QAM) and orthogonal frequency-division multiplexing (OFDM) modulation. Singh et al. [9] have analyzed the performance of the OFDM technique in tropical weather conditions of India. They have collected the data from the Indian Meteorological Department for potential regions in India, comprising the coastal and inland locations, for calculating the specific rain attenuation coefficient. The usage of modulation techniques depends on the technical availability and necessity. Many modulation techniques require external modulators, which aren't cheap and require complex setups. Some modulation techniques do not require external modulators; one such technique is OOK, which is the most basic modulation technique.

Various mitigation techniques are being designed in order to increase the quality of the communication link. One of the most common mitigation techniques is aperture averaging, which reduces the impact of beam fluctuations by using a larger receiving area, and was reported by Fernandes et al. [6]. They have mainly focused on beam alignment in order to increase the SNR at the receiver. The second technique is spatial diversity, which uses multiple beams (Multiple Input) or receivers (Multiple Output) to increase the chances of receiving a strong signal. Li et al. [10] used full duplex Multiple Input Multiple Output (MIMO) communication channels to transfer data; Wang et al. [11] used large scale MIMO for 6G communication; Elsayed et al. [12] used advanced diversity multiplexing with hybrid N-SM/OMI M-ary spatial pulse-position modulation schemes in order to mitigate the atmosphere turbulence faced in MIMO-RF/FSO DWDM systems and also investigated the performance of modified OOK and adaptive threshold for wavelength division multiplexing free-space optical systems impaired by inter-channel crosstalk, atmospheric turbulence, and amplified spontaneous emission (ASE) noise [13]; Naila et al. [14] used linear array design to evaluate conventional imaging in optical wireless communication (OWC) using MIMO; and Gu et al. [15] used Time Delay Signature Suppressing and developed a Security-Enhanced Electro-Optic Mutual Injection Secure Communication Scheme and a synchronous chaotic and electro-optic self-feedback dual-phase encryption-based high-speed physical layer secure communication scheme [16]. The most adaptive optics can adjust the beam in real time to compensate for distortions in the atmosphere by using waveform sensors and deformable mirror sensors. Stotts and Andrews [17] used an adaptive optics model to characterize turbulence mitigation for the FSOC link, and Xu et al. [18] designed a Nadam SPGD Algorithm for Sensor-Less Adaptive Optics in Coherent FSOC.

As FSOC is a line-of-sight (LOS) communication, the critical challenge in it is maintaining a precise alignment between the transmitter and receiver, especially in scenarios involving mobile platforms such as unmanned aerial vehicles, satellites, or moving ground terminals. Due to the tiny beam divergence of optical signals, even small misalignments might cause the communication link to completely fail or significantly lose signals [19]. Advanced beam steering and tracking systems with real-time adjustment capabilities are needed for FSOC devices to get around this. These systems frequently use motors, gimbals, or quick steering mirrors to dynamically adjust for the variations [19, 20].

Further, the development of advanced atmospheric testbeds allows for the simulation of real-world weather conditions, enabling researchers to study how FSOC performs under various environmental effects [1]. These testbeds replicate the challenges that FSOC systems would face when deployed in actual operating conditions, such as urban environments or remote areas. By evaluating FSOC systems in these simulated conditions, researchers can identify the most effective strategies for maintaining high performance and minimizing signal degradation [21, 22].

In this study, we aim to evaluate the performance of RSA encryption in FSOC using a controlled environment (chambers) where we simulate various atmospheric effects like fog, smoke, and wind, and we use a clear channel as our reference channel to compare these effects and transfer files between the transmitter and the receiver. RSA encryption has been clubbed with modulation schemes, namely, OOK-NRZ and PPM, and their combined performance is also evaluated in the same conditions. This helps us in analyzing the reliability of the secured link, which is calculated by the error fraction, which gives an idea of the possibility of FSOC being used in real time for various applications.

2. Theoretical Framework

2.1. Channel modeling

Channel modeling is often essential for investigating the performance of the FSOC channel. Several reports suggest that variations in the channel can directly affect the SNR and BER and the performance of the links [23–29]. The free-space channel plays a pivotal role in determining the effectiveness of information transfer between the transmitter and receiver. The reliability of communication is directly influenced by channel parameters such as absorption and scattering due to fog, smoke, and crosswinds. We carried out basic simulations before the testbed communication experiments. The link performance simulations were carried out from the estimated experimental attention coefficients. This allows a direct comparison of the experiment and the simulation results. We have calculated the probability of error with the communication range and the SNR for all the fog, smoke, wind, and a clear channel. The standard terms, like noise addition and the propagation loss, were used while carrying out the simulations.

For the propagation loss, a free-space path loss, L_p, is defined as:

$$L_p \triangleq \frac{1}{4\pi r^2} \tag{1}$$

Channel attenuation loss, L_t, is defined as:

$$L_t = e^{-\alpha_t r} \tag{2}$$

where:
r is the communication range.
α_t is the total attenuation coefficient.
The total channel attenuation, L_c, is given by:

$$L_c = L_p L_t \tag{3}$$

Using these losses, the SNR can be modeled as:

$$\mathrm{SNR} = \frac{P_1 \cdot e^{-\alpha_t r} \cdot D^2}{4r^2 \cdot \tan^2(\Theta_0) \cdot \mathrm{NEP}} \tag{4}$$

where:
P_1: Transmitter optical power,

Figure 1
BER versus SNR for different modulation schemes under (a) fog and (b) smoke

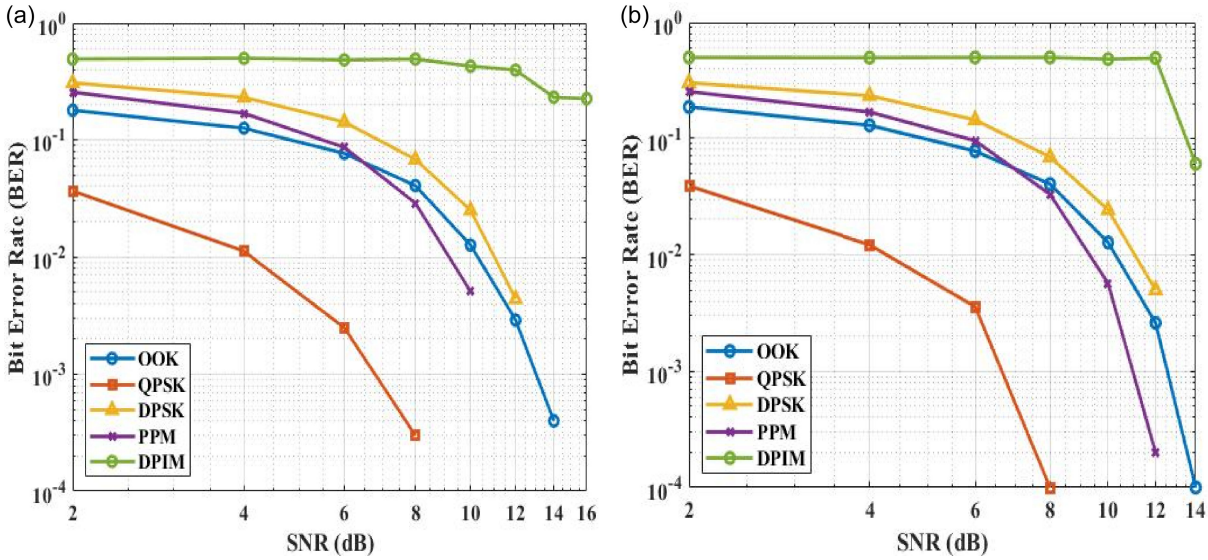

D: Receiver aperture diameter,

Θ_0: Angle between the optical axis and the LOS,

NEP: Noise-equivalent power—a metric representing the combined effect of various noise sources.

The NEP is defined as the **root mean square** sum of background noise, shot noise, thermal noise, and dark current noise, all of which affect the signal at the detection or processing stage.

Figure 1 shows the BER performance versus SNR for different modulation schemes under two adverse atmospheric conditions: (a) fog and (b) smoke in the FSO channel. Across both scenarios, Quadrature Phase-Shift Keying (QPSK) consistently performs better than the other modulation schemes by offering the lowest BER at all SNRs. In Figure 1(a) for fog, QPSK drops well below 10^{-3} at high SNRs (above 12 dB), while OOK, DPSK, and PPM follow with slightly higher error rates. DPIM shows poor performance under fog, retaining a higher BER even at high SNRs. In Figure 1(b) for smoke, QPSK maintains its strong performance, with its BER falling faster than OOK, DPSK, and PPM as SNR increases. DPIM, meanwhile, performs the worst in both conditions, reflecting its greater vulnerability to atmospheric attenuation. Overall, fog introduces less degradation than smoke, as the respective BER drops more slowly under smoke for all modulation schemes, demonstrating a greater impact of smoke-related scattering on optical communication.

In optical communication, modulation schemes like OOK-NRZ, OOK-RZ, DPIM, and PPM each offer unique trade-offs in power and spectral efficiency, as well as system complexity. Each scheme is selected based on the specific requirements of the optical system, balancing power efficiency, spectral efficiency, and implementation complexity. Encryption is based on algorithms that scramble information into unreadable and unscrambleable forms. Encryption changes the input data and makes it more complex, which in turn can affect the efficiency of modulation schemes. In this context, we will discuss the effect of the channel on modulation schemes when encrypted data is sent.

2.2. Modulation schemes

OOK-NRZ encodes binary data as the presence (1) or absence (0) of light in a continuous waveform, without resetting to a baseline between bits. This makes it spectrally efficient, as the signal occupies minimal bandwidth, and is easy to implement with simpler transmitters and receivers. However, it is prone to inter-symbol interference (ISI) at high data rates since there is no return to a baseline to help differentiate consecutive bits. Its moderate power efficiency makes it a widely used scheme for optical links operating at lower to medium data rates [1, 29].

OOK-RZ also represents binary data as light pulses but differs by returning to a baseline within each bit interval. This resetting reduces ISI and improves system performance, particularly for timing recovery and clock synchronization. However, the added resetting process results in lower spectral efficiency and increased power consumption since the transmitter must turn on and off more frequently [1, 3, 30]. In the DPIM, data is encoded in the time interval between consecutive pulses. Unlike traditional schemes that encode data in the amplitude or presence of a signal, DPIM focuses on varying the time gap between pulses to represent binary data. This approach improves power efficiency by concentrating energy into discrete time intervals. While DPIM offers advantages in terms of robustness to noise and signal degradation, it typically requires more complex timing synchronization and may result in reduced spectral efficiency compared to other modulation schemes like OOK. It is suitable for systems where power efficiency is prioritized over bandwidth utilization [31–33].

PPM encodes information in the time slot position of a single pulse within a frame. PPM achieves exceptional power efficiency because energy is concentrated into narrow pulses, which is advantageous in photon-limited or long-distance communication systems. However, this comes at the expense of spectral efficiency, as it requires larger bandwidths to represent the same data rate. Moreover, the complexity of generating and detecting PPM signals, along with stringent synchronization requirements, makes it less practical for some systems [34, 35].

Along with the abovementioned modulation schemes, there are various other kinds of modulation techniques. One of them is phase modulation, as the name suggests, where the phase of the signal is altered to transfer data. This technique offers improved noise immunity, enhanced transmission bandwidth, and data rates. A wide range of phase modulation techniques is used in the FSO channel. Phase-Shift Keying techniques like DPSK, QPSK, etc., are very popular due to their spectral efficiency.

Figure 2
Block diagram of the RSA algorithm

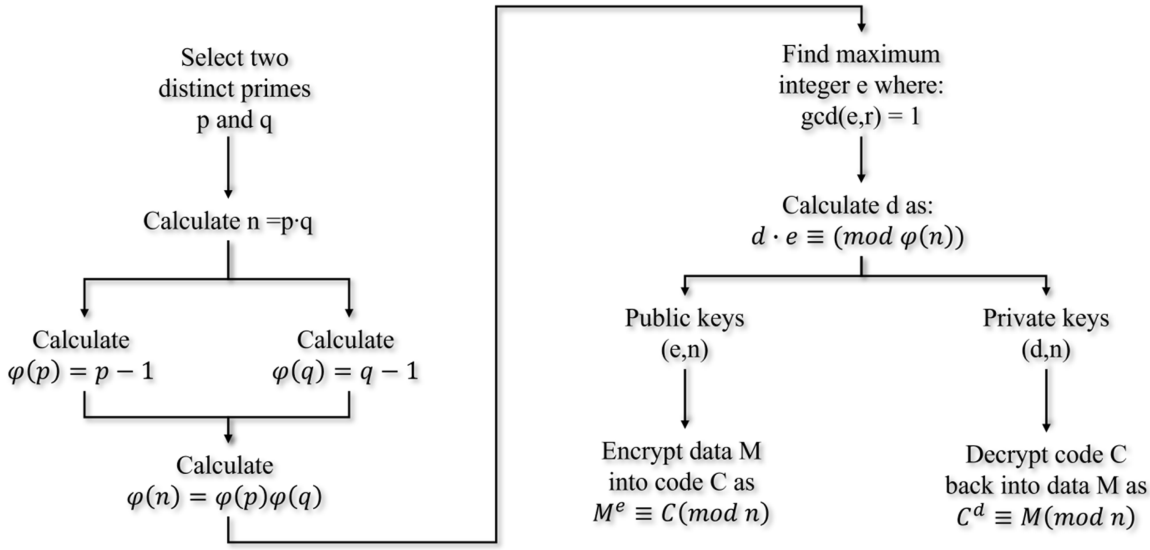

DPSK is a non-coherent phase modulation technique in which the information is encoded in the relative phase change between successive symbols instead of their absolute phase. DPSK is more power efficient and has a simpler receiver, as there is no requirement for carrier phase recovery, and is less complex compared to coherent schemes. However, QPSK is a coherent phase modulation scheme in which each symbol carries two bits, which can be achieved by varying the phase of the carrier among four distinct values—0°, 90°, 180°, and 270°—thus resulting in a more spectrally efficient system. The 2 bits per symbol, that is, higher spectral efficiency, allows for higher data throughput. QPSK is a bit complex compared to DPSK as it requires phase synchronization, which is compensated by its spectral efficiency [3, 36].

In FSOC systems, atmospheric conditions significantly influence performance. Clear weather provides optimal conditions with minimal signal attenuation and high reliability. Fog, consisting of dense water droplets, causes severe attenuation due to Mie scattering, drastically reducing signal strength and range. Smoke, made up of fine particulate matter, scatters and absorbs light, leading to moderate signal degradation [37, 38]. Wind-induced channel jittering creates beam misalignment and angular deviations, impairing signal reception and stability. These conditions collectively impact FSOC by reducing signal strength, increasing error rates, and limiting communication range and reliability, necessitating robust design and adaptive technologies to mitigate their effects [39–41].

2.3. Overview of encryption techniques

Security is a critical aspect in any communication field; it holds a prominent value in FSOC too, particularly as it becomes a contender for high-speed data transmission in defense, aerospace, and commercial sectors. As the optical sources have a tiny beam divergence, the beam width is too narrow, which makes it difficult to intercept without LOS access. Encryption techniques can be used to increase the security of the communication link; they are essential to maintain data confidentiality and integrity. There are mainly two types of encryption techniques that can be integrated into FSOC; they are symmetric encryption, such as AES, and asymmetric encryption, such as RSA. Symmetric encryption is used in high-throughput scenarios due to its speed and lower computational overhead, whereas asymmetric encryption is used for secure key exchange [42–45]. The inclusion of encryption protocols at the physical layer ensures end-to-end secure communication over atmospheric optical channels.

Symmetric encryption techniques use the same key for encrypting and decrypting the messages; they are well known for their speed and efficiency in FSOC. AES and Data Encryption Standard (DES) are the most commonly used symmetric encryption techniques. AES and DES are from the same sub-category of symmetric encryption, that is, Block Ciphers.

The DES was developed in the 1970s and was used widely in digital communications. It used to operate with a block size of 64 bits and a key size of 64 bits, where 56 bits were the actual key and 8 bits were added for parity. The AES was developed in 2001 and was developed mainly to replace DES due to security reasons. AES is widely used in communication due to its resistance to known attacks and throughput. AES operates with a block size of 128 bits and has three available key sizes, 128, 192, and 256 bits, each having a different number of rounds, 10, 12, and 14, respectively.

The RSA algorithm is an asymmetric cryptographic method used for secure communication, relying on a pair of public and private keys. It begins with key generation by selecting two large prime numbers, p and q, and computing their product $\mathrm{n} = \mathrm{p} \cdot \mathrm{q}$, which forms the modulus. Euler's totient function $\varphi(\mathrm{n}) = (\mathrm{p} - 1) \cdot (\mathrm{q} - 1)$ is calculated, and a public exponent e is chosen such that $1 < e < \varphi(\mathrm{n})$ and e is coprime with $\varphi(\mathrm{n})$. The private key exponent d is then computed as the modular multiplicative inverse of e modulo $\varphi(\mathrm{n})$. For encryption, a plaintext message M is converted into ciphertext C using $\mathrm{C} \equiv \mathrm{M}^{\mathrm{e}} \pmod{\mathrm{n}}$. For decryption, the private key is applied to retrieve M from C using $\mathrm{M} \equiv \mathrm{C}^{\mathrm{d}} \pmod{\mathrm{n}}$. Figure 2 depicts the algorithm involved in the RSA encryption and decryption as described above. The security of RSA relies on the computational difficulty of factoring large composite numbers [45].

2.4. Simulations

The FSOC channel can be characterized as the Additive White Gaussian Noise (AWGN) channel. We took an encrypted text file

Figure 3
Bit error rate (BER) versus communication range under various atmospheric conditions for (a) NRZ, (b) RZ, (c) PPM, (d) DPIM, (e) QPSK, and (f) DPSK modulation schemes and 5 mW laser

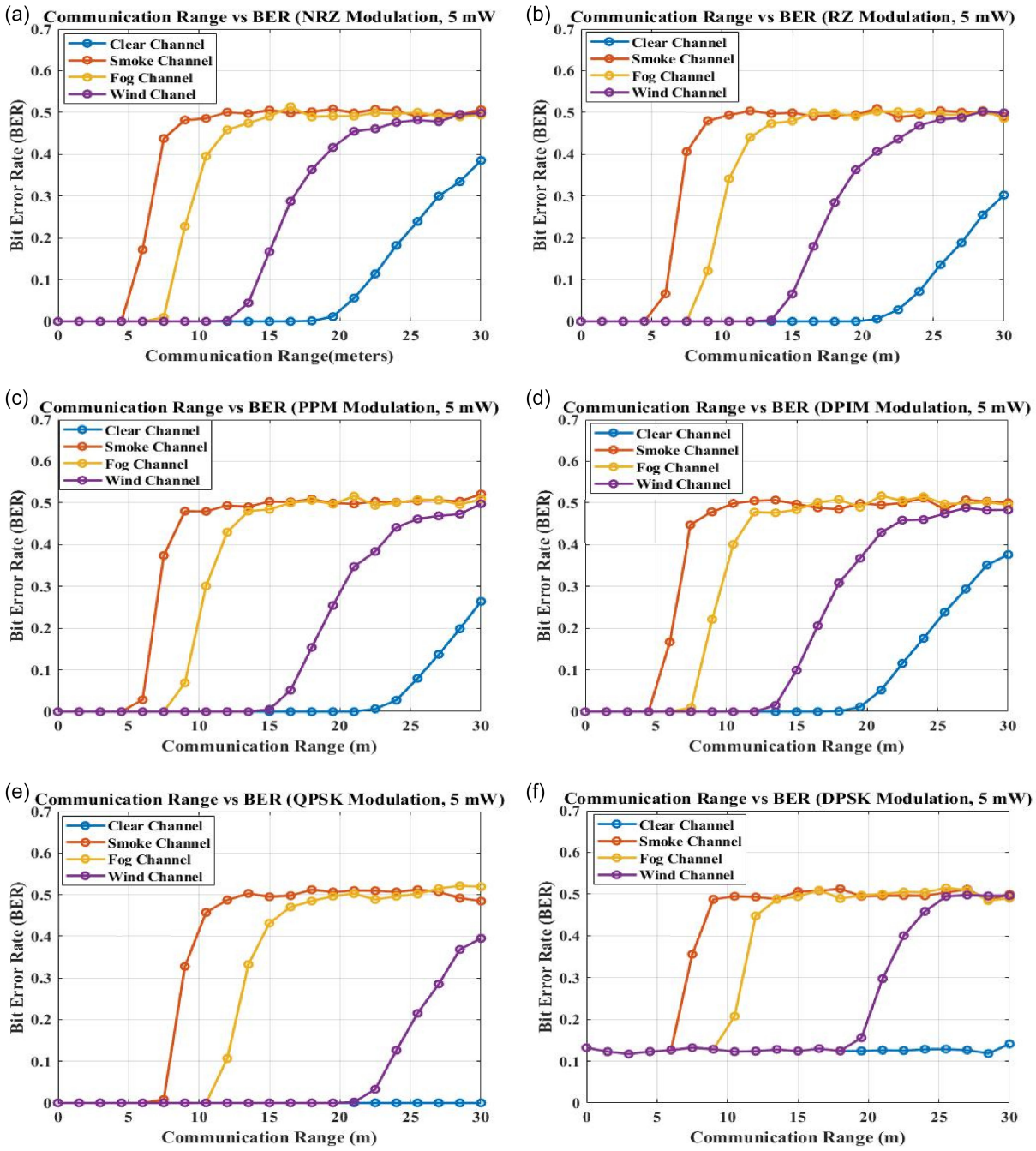

and converted it into bits; these bits act as source information, which is modulated as per the mentioned modulation schemes. The FSOC channel can be described as an AWGN channel. We took an encrypted text file and converted it into bits, which serve as the source information. These bits are then modulated according to the specified modulation schemes and transmitted through the AWGN channel. The channel introduces noise and signal attenuation, which can be quantified by the SNR derived from the channel characteristics. Passed through the AWGN channel, which introduces the noise and signal attenuation as by SNR, which is derived using channel characteristics as shown in Equation (4). For **n** bits, BER can be written as:

$$BER = \frac{\sum_{i=0}^{n} \mathrm{XOR}(Tx_i,\ Rx_i)}{n} \tag{5}$$

Figure 3 illustrates the BER performance over varying communication ranges under different environmental channel conditions (clear, smoke, fog, and wind) and for various modulation schemes at a fixed transmission power of 5 mW. Figure 3(a) shows that for NRZ modulation, the BER increases significantly in the presence of fog and smoke, reaching near 0.5 and above at short ranges (~5–10 m), while the clear channel maintains very low BER up to 30 m. The wind channel shows moderate BER degradation. Figure 3(b) indicates that RZ

Figure 4
Overall block diagram of the hardware setup, where m(t) is the information, x(t) is the optical signal, n(t) is the noise due to atmospheric channels, and y(t) is the decoded data

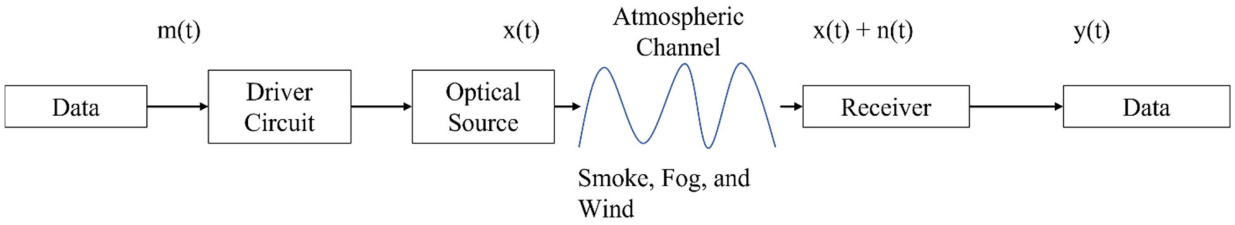

modulation performs similarly to NRZ but shows slightly better resilience under windy conditions, though fog and smoke still lead to a high BER at short distances. Figure 3(c) demonstrates that PPM modulation provides slightly better performance than NRZ and RZ in windy environments, with BER rising more gradually. However, smoke and fog still deteriorate performance rapidly. Figure 3(d) highlights that DPIM modulation performs comparably to PPM, with a more gradual BER increase in the wind channel, indicating its relative robustness to moderate turbulence. Figure 3(e) reveals that QPSK modulation provides superior performance, maintaining a very low BER in both clear and windy conditions, even up to 30 m. However, smoke and fog still result in high BER early on (~5 m). Figure 3(f) shows that DPSK modulation offers good performance under wind and clear conditions, similar to QPSK, with BER staying below 0.1 up to long distances. However, fog and smoke cause the BER to saturate around 0.5, indicating performance degradation in dense scattering environments. The clear oversight is that QPSK and DPSK stand out as the most reliable modulation techniques under all tested channel conditions, especially for longer communication ranges. However, requires an external modulation scheme.

3. Experimental Setup

The main challenge in investigating the atmospheric effects is to simulate those mimicking conditions in a lab scale with a controlled environment. For this purpose, we have developed various atmospheric testbeds: for wet fog, dry smoke, a wind channel (with cross flow), and a clear channel for control. All the chambers will have a length of 2 m and 30 cm × 30 cm. The purpose of these chambers is to maintain a consistent environment till we complete the data recording of the proposed experimental setup. The schematic is shown in Figure 4, and the actual experimental setup photographs are shown in Figure 5. The different simulated conditions are fog, smoke, and wind channel (jittering), along with clear conditions for comparison. The receiver power is measured to be around 75 − 100 uW using a power meter.

The fog chamber uses an ultrasonic humidifier to create fog by converting water into mist with high-frequency vibrations and high-rpm fans to pump the fog into the chamber, while temperature control reduces moisture. For our smoke chamber, we use a high-speed fan to evenly disperse smoke particles, which scatter and absorb light, reducing its intensity as it passes through. For the wind tunnel, we create turbulence by blowing air in perpendicular directions with high-speed fans, causing jitter in the light passing through due to changes in the air's refractive index. The experimental setup consists of an optical source (laser diode), which will be modulated as per the incoming data stream, and travels through the simulated adverse conditions. RSA encryption will be chosen

Figure 5
Experimental setup consisting of Tx and Rx PCs, laser, photodetector, and power meter in (a) smoke channel, (b) wind channel, and (c) fog channel

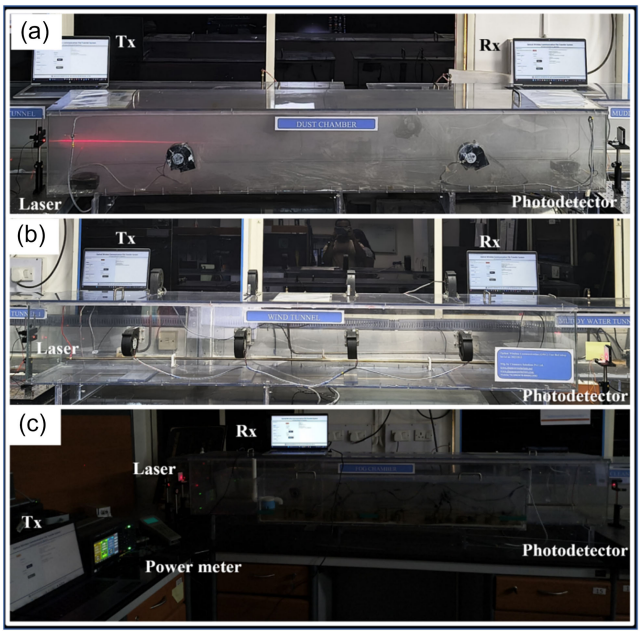

while selecting the data file and decoded back only with the correct public keys and private keys. We also had the option of choosing the data rates. Once the data was transferred under the abovementioned conditions, with the choice of data rate, the receiver section correctly decrypts, decodes the modulation, and stores the data in the receiver PC. We compare the same with the original file and calculate the percentage error fraction by comparing the binary bit streams. The clear atmospheric channel is used as a reference to understand the effects of the simulated adverse atmospheric conditions.

An in-house developed graphical user interface (GUI), as seen in Figure 6 using PYTHON, has been used for data transfer; the GUI is capable of handling all types of data (.mp3, .mp4, .txt, .jpg, etc.), and the data will be broken down into binary format ready for transmission. This binary stream is fed into the 5 mW laser, which will modulate accordingly. That is, if the bit is "1," the laser will be at the ON state, and it'll be at the OFF state if the bit is "0"; the frequency of this modulation depends on the data rate chosen in the GUI—for example, if the chosen data rate is 9600 bps, the laser modulates 9600 times per second. The GUI also provides an option to choose

Figure 6
Graphical user interface (GUI) developed in-house for file transfer

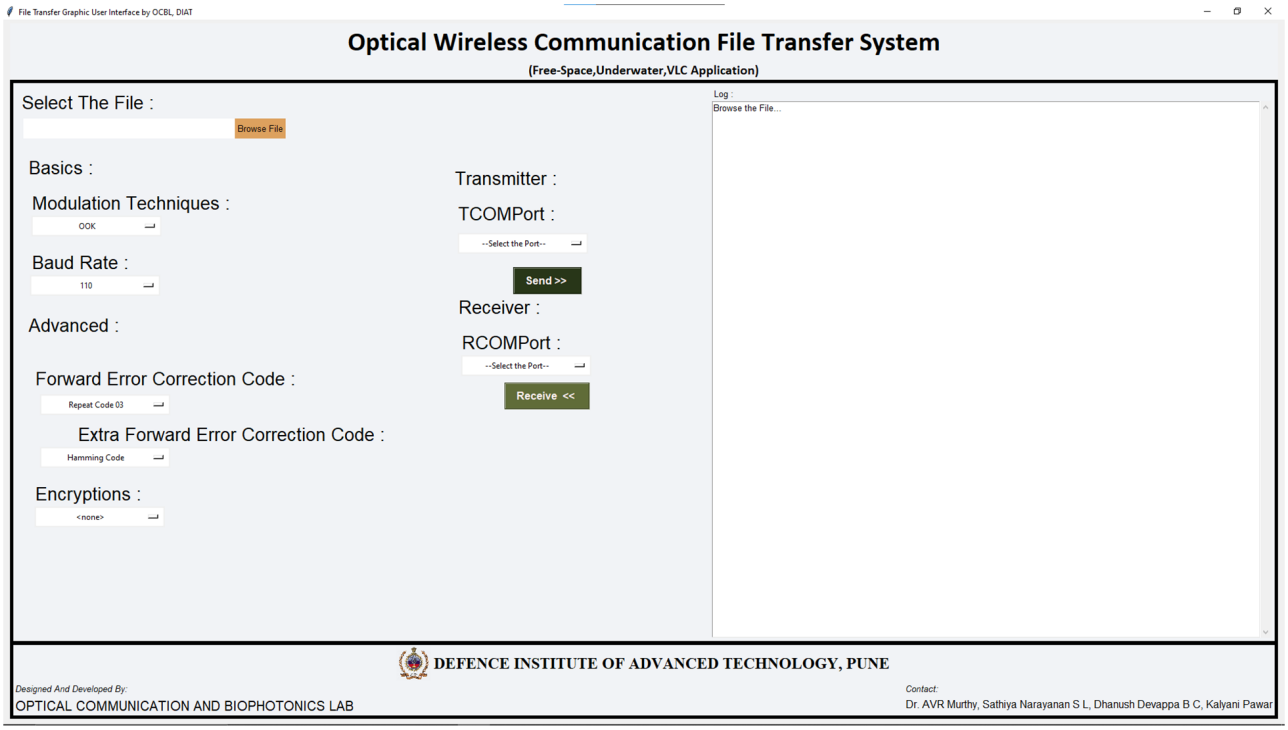

the appropriate modulation technique (OOK-NRZ, OOK-RZ, PPM, and DPIM) as per the requirement, and the usage of RSA encryption is also a choice. To feed the data from the PC into the laser, we will have to convert the data from digital signals to electrical signals using a USB to TTL adapter, which can be easily plugged into the PC. The data from the TTL output will be passed through a bias-tee circuit to amplify the signal and drive the laser. The transmitted data will be received using a photodetector, which will convert the optical signals into electrical signals. These electrical signals are converted back into digital signals using a USB to TTL adapter for the PC to read. The data in the binary stream is reconstructed back into its original format.

The experiment is conducted with varying parameters; for example, we have obtained the execution time values by varying the data rate while keeping the encryption strength constant—that is, the prime numbers used are constant ($p = 47$ and $q = 53$) when the RSA encryption has been applied. Similarly, while keeping the data rate constant (9600 bps), we obtained execution time values by varying the encryption strength (p and q values). Their respective error fractions have also been calculated using Equation (6).

$$Error\ Fraction = \frac{Total\ number\ of\ error\ bits\ in\ received\ file}{Total\ number\ of\ bits\ in\ transmitted\ file} \quad (6)$$

4. Results and Discussions

4.1. Effect of RSA encryption on different modulation schemes

As stated in the previous sections, we have conducted numerous experiments and analyses of secure FSOC links with different adverse atmospheric conditions like fog, smoke, and wind under controlled chambers in order to simulate real-world scenarios. These data are analyzed with the rest and also with the data obtained from a clear channel, which is used for reference.

Using the data obtained by varying the data rates while keeping the encryption strength constant, we were able to procure the execution time, which has been plotted and shown in Figure 7. As we examine the graphs in Figure 7, we note that OOK-NRZ exhibits lower execution time compared to PPM, RZ, and DPIM at increasing data rates, making it more efficient for unencrypted transmission in FSOC. RSA encryption significantly increases execution time for all modulation schemes. This is due to the addition of bits to encrypt the data; the size of the additional bits (data size) depends on the encryption strength. Since we are using the same value of encryption strength in this experiment, the amount of increase in bits is constant for all the RSA encryption data. However, OOK-NRZ still maintains a relatively better performance at higher data rates.

On the other hand, if we keep the data rate as a constant value, that is, 9600 bps, and vary the encryption strength, we can see a trend in execution time, which is shown in Figure 8. The execution time remains constant for smaller sizes and starts to rise with larger encryption strength for all modulation schemes, indicating the computational overhead introduced by stronger encryption, meaning the higher the encryption, the larger the increase in data, which creates difficulty for a third party to decrypt without the private key. Here too, OOK-NRZ has a lesser execution time as compared to the other three modulations for the same value of encryption strength. The execution time of the smoke channel and fog channel increases more than that of the clear channel. This is due to the degradation of the signal through the channel, which causes errors, because of which the decryption isn't performed perfectly, creating irregularities in the execution time. This indicates that OOK-NRZ is comparatively better at higher

Figure 7
Execution time (s) versus data rate (Mbps) for OOK-NRZ, PPM, OOK-RZ, and DPIM (a, c, e, g) with and (b, d, f, h) without RSA encryption, respectively, where the prime numbers for RSA encryption are p = 47 and q = 53

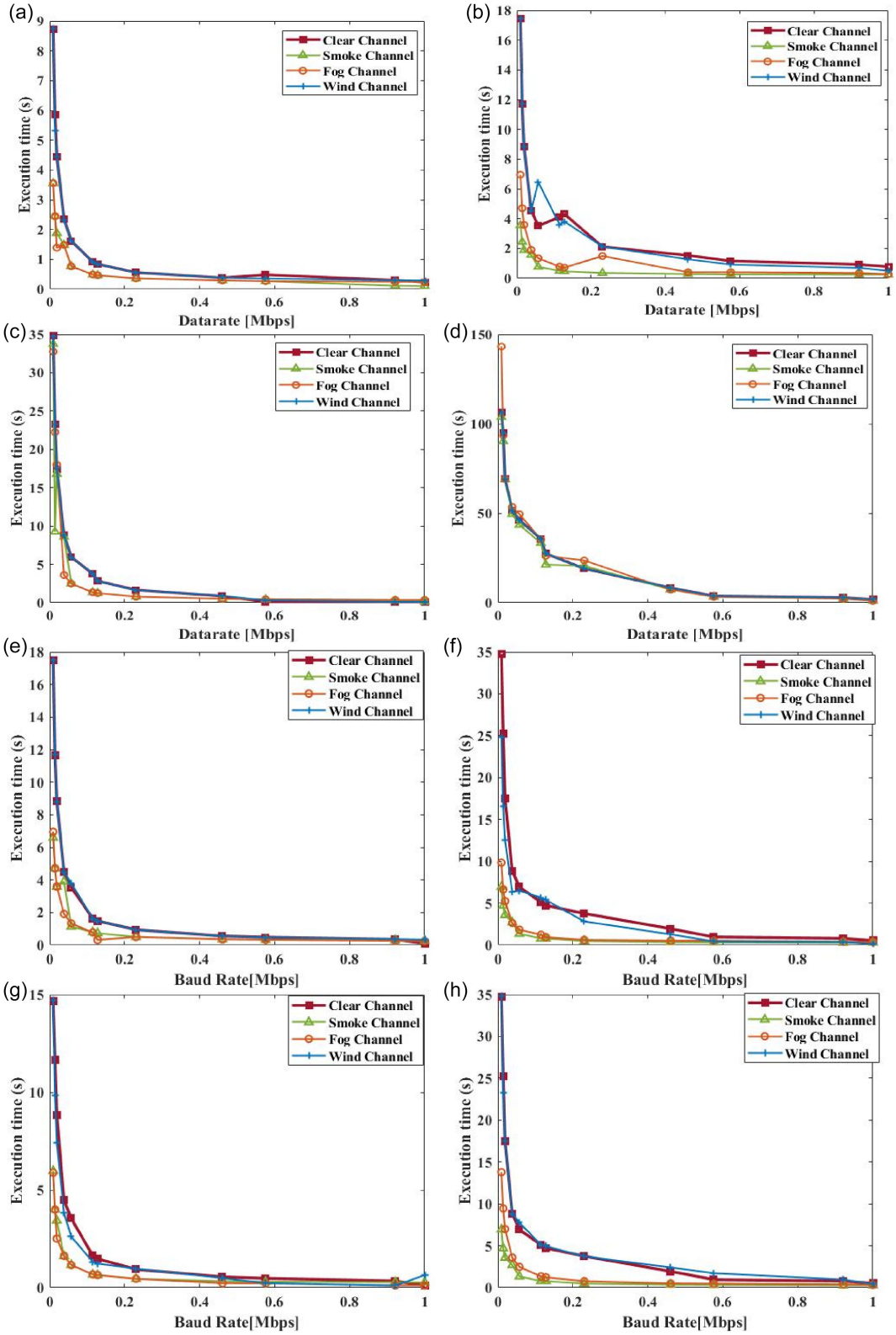

Figure 8
Execution time (s) versus encryption strength at 9.6 kbps for (a) OOK-NRZ, (b) PPM, (c) OOK-RZ, and (d) DPIM

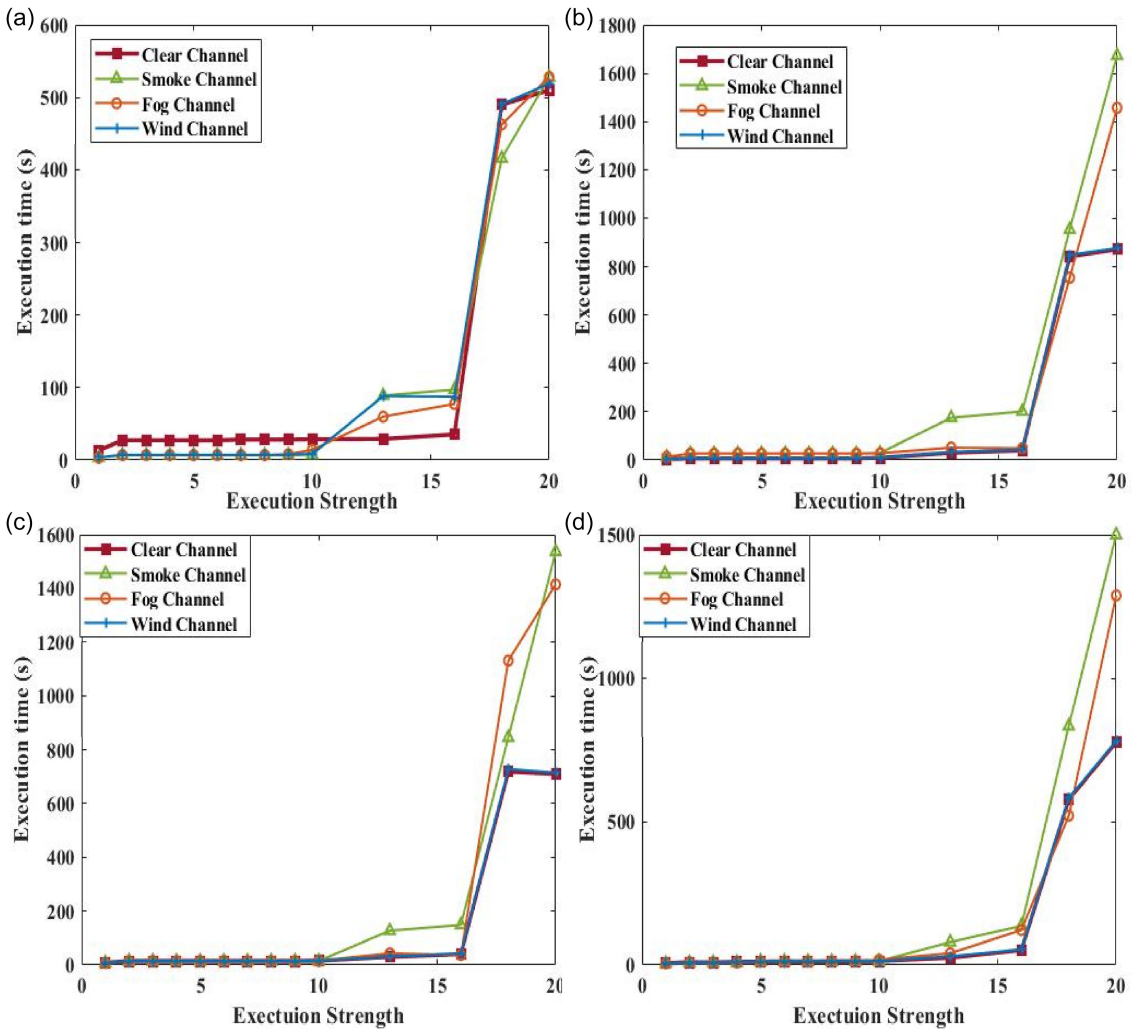

encryption strengths compared to PPM, RZ, and DPIM modulation schemes, as they increase the number of bits, which can be susceptible to loss in data at adverse atmospheric conditions.

4.2. Link performance and evaluation of secure FSOC

After confirming the successful implementation of RSA in the FSOC link, we have evaluated the link performance by analyzing the received data with the original data and calculating the percentage error fraction. This was conducted in two dimensions, with different data rates and with different encryption strengths for all modulation formats and for all adverse conditions.

The data from Figure 9 shows the error fraction versus data rate for all scenarios. From the graphs in Figure 9, we observe that the OOK-NRZ modulation shows a lower error fraction than PPM, RZ, and DPIM at lower data rates. As the data rate increases, error rates for all modulation schemes rise, but PPM is seen to suffer more degradation, followed by DPIM and OOK-RZ. Also, the fog and smoke suffer more errors for every modulation format. This is associated with the increased scattering phenomenon. Cross and clear wind did not create much deterioration compared to the clear channel. We further investigate the graphs and find that encryption increases the error fraction for both schemes. The OOK-NRZ modulation showed superior error performance over PPM, RZ, and DPIM, though the gap narrows. Larger encryption strengths worsen the error fraction for all modulation schemes, but PPM displays a higher sensitivity to the key size, as shown in Figure 10.

We can draw some conclusions from our earlier observations. We find that the OOK-NRZ modulation is more suitable due to its lower execution time and error fraction, particularly at higher data rates. The OOK-NRZ modulation is also observed to outperform PPM, RZ, and DPIM under RSA encryption for both execution time and error performance, especially with large encryption strengths. However, PPM and DPIM can be preferred for better energy efficiency, though their error performance degrades more rapidly with increasing data rates and encryption overhead.

5. Conclusion and Future Scope

This study focuses on the performance of secure FSOC for real-world applications by simulating various atmospheric conditions in a testbed and the integration of advanced modulation techniques to enhance data rates and improve bandwidth efficiency. Future possibilities can include the system's improved stability through the application of adaptive optics, which can compensate dynamically

Figure 9
Error fraction versus data rate (Mbps) for OOK-NRZ, PPM, OOK-RZ, and DPIM (a, c, e, g) with and (b, d, f, h) without RSA encryption, respectively, where the prime numbers for RSA encryption are p = 47 and q = 53

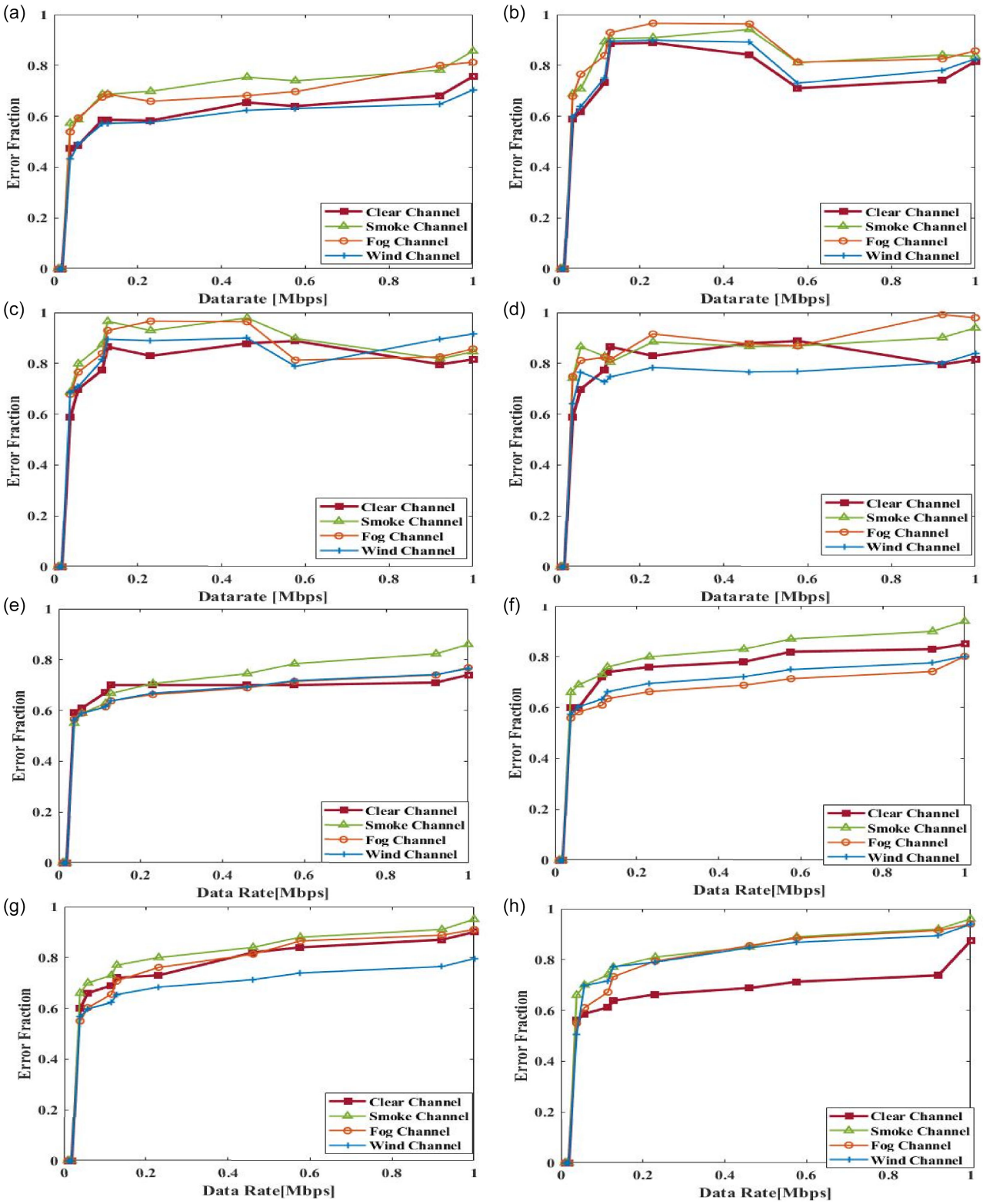

for atmospheric disturbances to provide a more stable and better-quality signal. Another important approach is the implementation of MIMO and SIMO (Single Input Multiple Output), which can increase the data rate and reliability by using several optical beams or detectors. These technologies can overcome the effects of signal degradation due to turbulence and other environmental factors, optimizing the communication link. A more robust and secure FSOC system can be developed by combining RSA encryption

Figure 10
Error fraction versus encryption strength for (a) OOK-NRZ, (b) PPM, (c) OOK-RZ, and (d) DPIM with RSA encryption

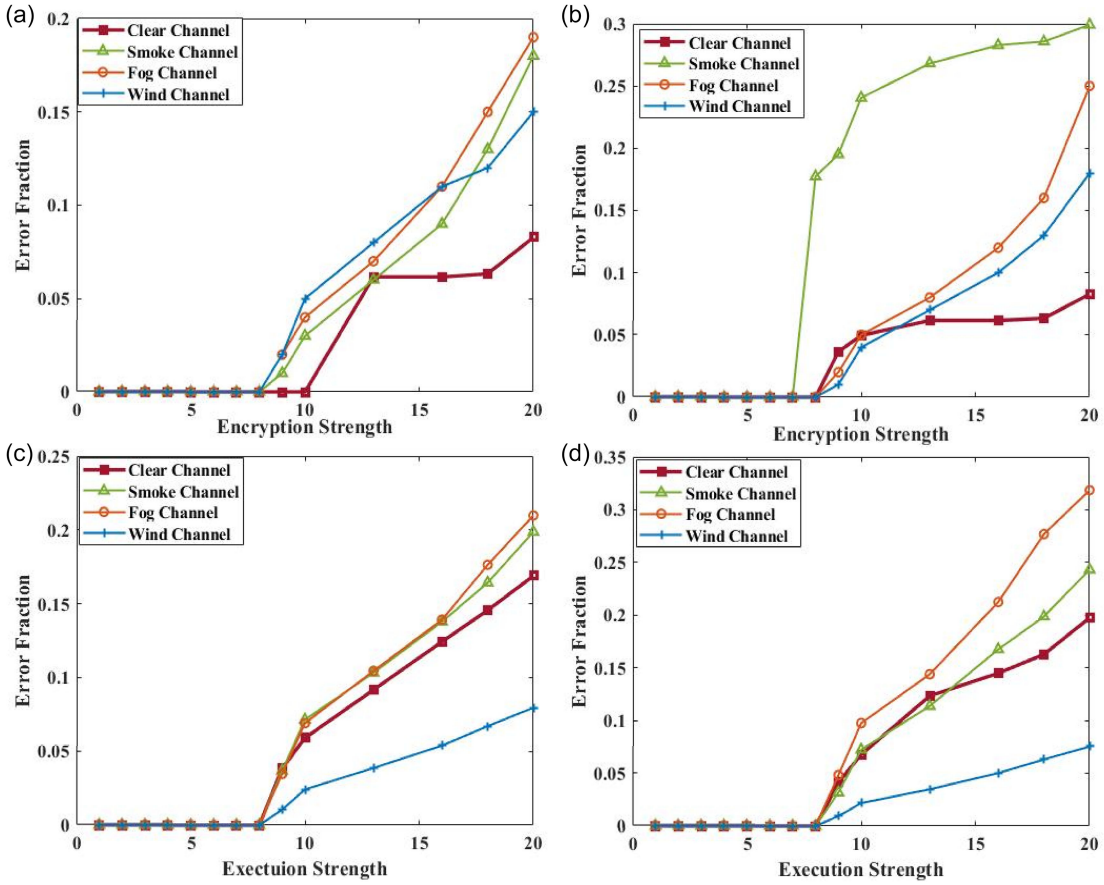

with adaptive optics and MIMO/SIMO configurations. By pursuing these strategies, FSOC systems can become more robust, efficient, and suitable for high-performance communication applications in dynamic and challenging environments.

Acknowledgment

All authors acknowledge the Defence Institute of Advanced Technology for financial and infrastructural support.

Ethical Statement

This study does not contain any studies with human or animal subjects performed by any of the authors.

Conflicts of Interest

The authors declare that they have no conflicts of interest to this work.

Data Availability Statement

Data are available from the corresponding author upon reasonable request.

Author Contribution Statement

Dhanush Devappa B C: Conceptualization, Methodology, Software, Formal analysis, Investigation, Data curation, Writing – original draft, Writing – review & editing, Visualization. **Chandani Kashyap:** Validation, Investigation, Data curation. **Shreyas Jain:** Validation, Formal analysis, Data curation, Writing – review & editing. **Soumit Banerjee:** Methodology. **Appala Venkata Ramana Murthy:** Conceptualization, Resources, Data curation, Writing – original draft, Writing – review & editing, Visualization, Supervision, Project administration.

References

[1] Sathiya Narayanan, S. L., Devappa B C, D., Pawar, K., Jain, S., & Venkata Ramana Murthy, A. (2024). Implementation of forward error correction for improved performance of free space optical communication channel in adverse atmospheric conditions. *Results in Optics*, *16*, 100689. https://doi.org/10.1016/j.rio.2024.100689

[2] Kaur, S., Kaur, J., & Sharma, A. (2023). Predicting the performance of radio over free space optics system using machine learning techniques. *Optik*, *281*, 170798. https://doi.org/10.1016/j.ijleo.2023.170798

[3] Bismi, B. S., & Azeem, S. (2023). Design and analysis of DPSK, QPSK modulations in underwater optical communication using free space optics. *Wireless Personal Communications*, *132*(2), 1487–1502. https://doi.org/10.1007/s11277-023-10671-2

[4] Chow, C.-W. (2024). Recent advances and future perspectives in optical wireless communication, free space optical communication and sensing for 6G. *Journal of Lightwave*

Technology, *42*(11), 3972–3980. https://doi.org/10.1109/JLT.2024.3386630

[5] Yao, H., Hao, Q., Chen, C., Li, L., Chang, Y., Du, S., . . . , & Jiang, H. (2022). Generation of temporal fading envelope sequences for the FSOC channel based on atmospheric turbulence optical parameters. *Optics Express*, *30*(19), 34519–34532. https://doi.org/10.1364/OE.465847

[6] Fernandes, M. A., Brandão, B. T., Georgieva, P., Monteiro, P. P., & Guiomar, F. P. (2021). Adaptive optical beam alignment and link protection switching for 5G-over-FSO. *Optics Express*, *29*(13), 20136. https://doi.org/10.1364/OE.426551

[7] Sinha, S., & Kumar, C. (2023). Performance evaluation of higher order modulation in FSOC system using homodyne detector. In *2023 International Conference on Recent Advances in Electrical, Electronics & Digital Healthcare Technologies*, 658–661. https://doi.org/10.1109/REEDCON57544.2023.10150482

[8] Sangeetha, R. G., Hemanth, C., & Jaiswal, I. (2022). Performance of different modulation scheme in free space optical transmission – A review. *Optik*, *254*, 168675. https://doi.org/10.1016/j.ijleo.2022.168675

[9] Singh, H., Mittal, N., & Singh, H. (2022). Evaluating the performance of free space optical communication (FSOC) system under tropical weather conditions in India. *International Journal of Communication Systems*, *35*(18), e5347. https://doi.org/10.1002/dac.5347

[10] Li, T., Sun, Z., Wang, Y., Mai, J., & Xu, D. (2024). Simultaneous wireless power and data transfer system with full-duplex MIMO communication channels for underwater applications. *IEEE Transactions on Industrial Informatics*, *20*(4), 6382–6393. https://doi.org/10.1109/TII.2023.3345459

[11] Wang, P., Li, C., & Xu, Z. (2018). A cost-efficient real-time 25 Mb/s system for LED-UOWC: Design, channel coding, FPGA implementation, and characterization. *Journal of Lightwave Technology*, *36*(13), 2627–2637. https://doi.org/10.1109/JLT.2018.2819985

[12] Elsayed, E. E. (2024). Atmospheric turbulence mitigation of MIMO-RF/FSO DWDM communication systems using advanced diversity multiplexing with hybrid N-SM/OMI M-ary spatial pulse-position modulation schemes. *Optics Communications*, *562*, 130558. https://doi.org/10.1016/j.optcom.2024.130558

[13] Elsayed, E. E. (2024). Investigations on modified OOK and adaptive threshold for wavelength division multiplexing free-space optical systems impaired by interchannel crosstalk, atmospheric turbulence, and ASE noise. *Journal of Optics.* Advance online publication. https://doi.org/10.1007/s12596-024-01929-4

[14] Naila, C. B., Nakamura, T., Okada, H., & Katayama, M. (2022). Evaluation of conventional and imaging MIMO OWC systems using linear array design. *IEEE Photonics Journal*, *14*(5), 1–9. https://doi.org/10.1109/JPHOT.2022.3203424

[15] Gu, W., Gao, X., An, Y., Wang, A., Wang, Y., Qin, Y., & Gao, Z. (2023). Security-enhanced electro-optic mutual injection secure communication scheme with time-delay signature suppressing. *IEEE Photonics Journal*, *15*(3), 1–8. https://doi.org/10.1109/JPHOT.2023.3279282

[16] Gu, W., & Gao, X. (2024). High-speed physical layer secure communication scheme based on synchronous chaotic and electro-optic self-feedback dual-phase encryption. *Journal of Optics*, *26*(1), 015703. https://doi.org/10.1088/2040-8986/ad15ea

[17] Stotts, L. B., & Andrews, L. C. (2021). Adaptive optics model characterizing turbulence mitigation for free space optical communications link budgets. *Optics Express*, *29*(13), 20307–20321. https://doi.org/10.1364/OE.430554

[18] Xu, X., Li, Y., Huang, P., Ju, M., & Tan, G. (2022). Ber performance of UWOC with APD receiver in wide range oceanic turbulence. *IEEE Access*, *10*, 25203–25218. https://doi.org/10.1109/ACCESS.2022.3154892

[19] Pandey, P., Matta, G., & Agrawal, M. (2022). Effect of transmitter divergence-angle on the performance of underwater visible light communication system. *Optical and Quantum Electronics*, *54*(12), 802. https://doi.org/10.1007/s11082-022-04195-5

[20] Sun, N., Wang, Y., Zhu, H., Zhang, J., Du, A., Wang, W., . . . , & Liu, J. (2022). Self-alignment FSOC system with miniaturized structure for small mobile platform. *IEEE Photonics Journal*, *14*(6), 1–6. https://doi.org/10.1109/JPHOT.2022.3193112

[21] Pawar, K., Devappa B C, D., & Murthy, A. V. R. (2024). Performance of FSOC link establishment using scan/stare approach. In *2024 IEEE Pune Section International Conference*, 1–4. https://doi.org/10.1109/PuneCon63413.2024.10894832

[22] Kumar, S., & Sharma, N. (2022). Emerging military applications of free space optical communication technology: A detailed review. *Journal of Physics: Conference Series*, *2161*(1), 012011. https://doi.org/10.1088/1742-6596/2161/1/012011

[23] Majumdar, A. K., Siegenthaler, J., & Land, P. (2012). Analysis of optical communications through the random air-water interface: Feasibility for under-water communications. In *Laser Communication and Propagation through the Atmosphere and Oceans: Proceedings of SPIE*, 8517, 85170T. https://doi.org/10.1117/12.928999

[24] Luo, S., Miao, M., & Li, X. (2025). A multi-dimensional modulation format for spectral efficiency improvement of PPM system and its BER performance analysis in free-space optical communication. *Journal of Optics*, *27*(4), 045702. https://doi.org/10.1088/2040-8986/ad8c5a

[25] Karp, S., & Gagliardi, R. (1969). The design of a pulse-position modulated optical communication system. *IEEE Transactions on Communications*, *17*(6), 670–676. https://doi.org/10.1109/TCOM.1969.1090162

[26] Saeed, N., Almorad, H., Dahrouj, H., Al-Naffouri, T. Y., Shamma, J. S., & Alouini, M.-S. (2021). Point-to-point communication in integrated satellite-aerial 6G networks: State-of-the-art and future challenges. *IEEE Open Journal of the Communications Society*, *2*, 1505–1525. https://doi.org/10.1109/OJCOMS.2021.3093110

[27] Hayal, M. R., Elsayed, E. E., Kakati, D., Singh, M., Elfikky, A., Boghdady, A. I., . . . , & Nurhidayat, I. (2023). Modeling and investigation on the performance enhancement of hovering UAV-based FSO relay optical wireless communication systems under pointing errors and atmospheric turbulence effects. *Optical and Quantum Electronics*, *55*(7), 625. https://doi.org/10.1007/s11082-023-04772-2

[28] Arockia Bazil Raj, A., Arputha Vijaya Selvi, J., & Durairaj, S. (2015). Comparison of different models for ground-level atmospheric turbulence strength (C_n^2) prediction with a new model according to local weather data for FSO applications. *Applied Optics*, *54*(4), 802–815. https://doi.org/10.1364/AO.54.000802

[29] Darwesh, L., & Kopeika, N. S. (2020). Deep learning for improving performance of OOK modulation over FSO turbulent channels. *IEEE Access*, *8*, 155275–155284. https://doi.org/10.1109/ACCESS.2020.3019113

[30] Dwivedy, P., Dixit, V., & Kumar, A. (2023). Cooperative VLC system using OOK modulation with imperfect CSI. *Physica Scripta*, *98*(2), 025509. https://doi.org/10.1088/1402-4896/acb095

[31] Ghassemlooy, Z., Hayes, A. R., Seed, N. L., & Kaluarachchi, E. D. (2002). Digital pulse interval modulation for optical communications. *IEEE Communications Magazine*, *36*(12), 95–99. https://doi.org/10.1109/35.735885

[32] Tao, M., Guan, J., Peng, T., Li, S., Yu, S., Song, J., . . . , & Gao, F. (2021). Simultaneous realization of laser ranging and communication based on dual-pulse interval modulation. *IEEE Transactions on Instrumentation and Measurement*, *70*, 1–10. https://doi.org/10.1109/TIM.2021.3082990

[33] Azhdari, S. M. H., Mahmoodzadeh, A., Khishe, M., & Agahi, H. (2023). Pulse repetition interval modulation recognition using deep CNN evolved by extreme learning machines and IP-based BBO algorithm. *Engineering Applications of Artificial Intelligence*, *123*, 106415. https://doi.org/10.1016/j.engappai.2023.106415

[34] Yu, N., Wang, P., & Zhuang, Z. (2021). Design of digital pulse-position modulation system. *Journal of Physics: Conference Series*, 2093(1), 012030. https://doi.org/10.1088/1742-6596/2093/1/012030

[35] Tang, W., Wang, S., Xu, Y., & Yu, Z. (2022). The research process, application, and the future development of pulse-position modulation. *Journal of Physics: Conference Series*, *2384*(1), 012026. https://doi.org/10.1088/1742-6596/2384/1/012026

[36] Tang, X., Zhang, L., Sun, C., Chen, Z., Wang, H., Jiang, R., . . . , & Zhang, A. (2020). Underwater wireless optical communication based on DPSK modulation and silicon photomultiplier. *IEEE Access*, *8*, 204676–204683. https://doi.org/10.1109/ACCESS.2020.3037174

[37] Neary, P. L., Watnik, A. T., Judd, K. P., Lindle, J. R., & Flann, N. S. (2020). Machine learning-based signal degradation models for attenuated underwater optical communication OAM beams. *Optics Communications*, *474*, 126058. https://doi.org/10.1016/j.optcom.2020.126058

[38] Cheng, Q., Cui, S., Zhou, K., & Liu, D. (2020). Training-aided joint frame and frequency synchronization for free space optical communication signals with low OSNR. *Optics Communications*, *473*, 126046. https://doi.org/10.1016/j.optcom.2020.126046

[39] Guiomar, F. P., Fernandes, M. A., Nascimento, J. L., Rodrigues, V., & Monteiro, P. P. (2022). Coherent free-space optical communications: Opportunities and challenges. *Journal of Lightwave Technology*, *40*(10), 3173–3186. https://doi.org/10.1109/JLT.2022.3164736

[40] Bekkali, A., Fujita, H., & Hattori, M. (2022). New generation free-space optical communication systems with advanced optical beam stabilizer. *Journal of Lightwave Technology*, *40*(5), 1509–1518. https://doi.org/10.1109/JLT.2022.3146252

[41] Yue, S., Hu, G., Zhan, C., Zhang, Y., & Zhu, M. (2021). DOA estimation of a space-limited MIMO radar with high degree of freedom. *Journal of Physics: Conference Series*, *2093*(1), 012029. https://doi.org/10.1088/1742-6596/2093/1/012029

[42] Zhang, Q. (2021). An overview and analysis of hybrid encryption: The combination of symmetric encryption and asymmetric encryption. In *2021 2nd International Conference on Computing and Data Science*, 616–622. https://doi.org/10.1109/CDS52072.2021.00111

[43] Al Mamun, S., Mahmood, M. A., & Amin, M. A. (2021). Ensuring security of encrypted information by hybrid AES and RSA algorithm with third-party confirmation. In *2021 5th International Conference on Intelligent Computing and Control Systems*, 337–343. https://doi.org/10.1109/ICICCS51141.2021.9432174

[44] Fatima, S., Rehman, T., Fatima, M., Khan, S., & Ali, M. A. (2022). Comparative analysis of AES and RSA algorithms for data security in cloud computing. *Engineering Proceedings*, *20*(1), 14. https://doi.org/10.3390/engproc2022020014

[45] Devappa B C, D., Banerjee, S., Pawar, K., & Venkata Ramana Murthy, A. (2025). Practical realization and performance analysis of Rivest-Shamir-Adleman encryption for secure underwater optical communication. *Next Research*, *2*(2), 100225. https://doi.org/10.1016/j.nexres.2025.100225

How to Cite: Devappa B C, D., Kashyap, C., Jain, S., Banerjee, S., & Murthy, A. V. R. (2025). Performance Analysis of RSA Encrypted Secure Free-Space Optical Communication Link Under Adverse Atmospheric Conditions Implemented on a Testbed. *Journal of Optics and Photonics Research*. https://doi.org/10.47852/bonviewJOPR52026038